

Osteochondral regeneration using an oriented nanofiber yarn-collagen type I/hyaluronate hybrid/TCP biphasic scaffold

Shen Liu,^{1*} Jinglei Wu,^{2*} Xudong Liu,^{1*} Desheng Chen,³ Gary L. Bowlin,⁴ Lei Cao,⁵ Jianxi Lu,⁵ Fengfeng Li,¹ Xiumei Mo,² Cunyi Fan¹

¹Department of Orthopaedics, Shanghai Jiao Tong University Affiliated Sixth People's Hospital, 600 Yishan Road, Shanghai 200233, People's Republic of China

²Biomaterials and Tissue Engineering Laboratory, College of Chemistry and Chemical Engineering and Biological Engineering, Donghua University, Shanghai 201620, People's Republic of China

³Department of Orthopaedics, The General Hospital of Ningxia Medical University, Yinchuan 750004, China

⁴Department of Biomedical Engineering, Virginia Commonwealth University, Richmond, Virginia 23284-3067

⁵Shanghai Key Laboratory of Orthopaedic Implants, Department of Orthopaedics, Shanghai Ninth People's Hospital, Shanghai Jiaotong University School of Medicine, 639 Zhizaoju Road, Shanghai 200011, People's Republic of China

Received 2 January 2014; revised 9 March 2014; accepted 22 April 2014

Published online 7 May 2014 in Wiley Online Library (wileyonlinelibrary.com). DOI: 10.1002/jbm.a.35206

Abstract: Osteochondral defects affect both the articular cartilage and the underlying subchondral bone, but poor osteochondral regeneration is still a daunting challenge. Although the tissue engineering technology provides a promising approach for osteochondral repair, an ideal biphasic scaffold is in high demand with regards to proper biomechanical strength. In this study, an oriented poly(L-lactic acid)-*co*-poly(ϵ -caprolactone) P(LLA-CL)/collagen type I (Col-I) nanofiber yarn mesh, fabricated by dynamic liquid electrospinning served as a skeleton for a freeze-dried Col-I/Hyaluronate (HA) chondral phase (SPONGE) to enhance the mechanical strength of the scaffold. *In vitro* results show that the Yarn

Col-I/HA hybrid scaffold (Yarn-CH) can allow the cell infiltration like sponge scaffolds. Using porous beta-tricalcium phosphate (TCP) as the osseous phase, the Yarn-CH/TCP biphasic scaffold was then assembled by freeze drying. After combination of bone marrow mesenchymal stem cells, the biphasic complex was successfully used to repair the osteochondral defects in a rabbit model with greatly improved repairing scores and compressive modulus. © 2014 Wiley Periodicals, Inc. *J Biomed Mater Res Part A*: 103A: 581–592, 2015.

Key Words: osteochondral defect, electrospinning, yarn, biphasic composite

How to cite this article: Liu S, Wu J, Liu X, Chen D, Bowlin GL, Cao L, Lu J, Li F, Mo X, Fan C. 2015. Osteochondral regeneration using an oriented nanofiber yarn-collagen type I/hyaluronate hybrid/TCP biphasic scaffold. *J Biomed Mater Res Part A* 2015;103A:581–592.

INTRODUCTION

Osteochondral defects affect both the articular cartilage and the underlying subchondral bone. Poor graft integration at the chondral interface and degeneration of the cartilage were previously reported.¹ Nowadays, despite improved mechanisms for cartilage healing,^{2,3} novel surgical techniques,^{4,5} and modified autologous osteochondral grafting,^{6,7} the repair of osteochondral defect is still a daunting challenge for surgeons. Although the technology of tissue engineering incorporating scaffolds and cells to regenerate functional osteochondral complex provides a promising approach for osteochondral repair, the evolution of scaffolding to engineer osteochondral complex still needs further study.^{8,9}

To resist the native physiological loads, the osteochondral implant should be mechanically compatible to the native tissue.¹⁰ An ideal chondral phase is highly demanded of the implant with regard to proper biomechanical strength, to avoid the repair cartilage being thinner than the native cartilage as in the presently used scaffolds due to mechanical incompatibility.⁹ The sponge-like scaffolds, fabricated using native cartilage extracellular matrix (ECM) components by freeze-drying, usually lack sufficient mechanical properties to support joint function during tissue regeneration. Although a biphasic osteochondral scaffold holds the promise for repair of osteochondral defects, there is a great need to maintain sound mechanical compatibility in a controllable polymeric system.

This article was published online on 7 May 2014. An error was subsequently identified. This notice is included in the online and print versions to indicate that both have been corrected 12 July 2014.

*These authors contributed equally to this work.

Correspondence to: C. Fan; e-mail: fancunyi@126.com (or) X. Mo; e-mail: xmm@dhu.edu.cn

Contract grant sponsor: National Science Foundation of China; contract grant numbers: 51003058 and 81271999

Contract grant sponsor: Nanotech Foundation of Shanghai; contract grant number: 11nm0503100

Contract grant sponsor: Shanghai Municipal Commission of Science and Technology Program and Rising-Star Program; contract grant number: 13QH1401900

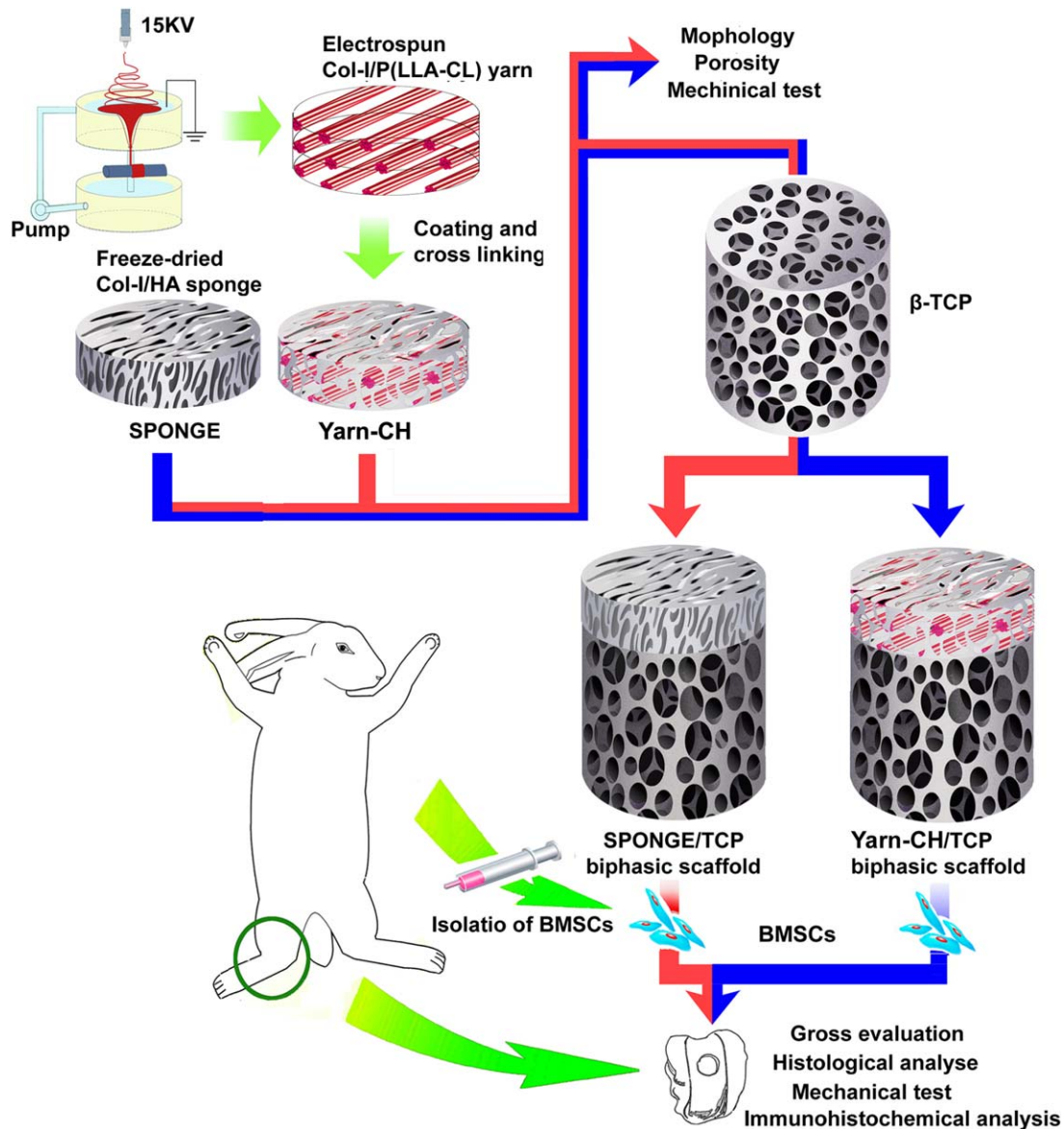


FIGURE 1. Oriented P(LLA-CL)/Col-I nanofiber yarn was fabricated by dynamic liquid electrospinning and subsequently used as the skeleton of the freeze-dried Col-I/HA chondral phase to reproduce some cartilaginous environmental cues, especially in the superficial zone. Then, porous beta-tricalcium phosphate was used as the osseous phase. After combining of the BMSCs, this tissue-engineered cartilage and TCP complex were used to repair osteochondral defects in the animal model. [Color figure can be viewed in the online issue, which is available at wileyonlinelibrary.com.]

A novel nanofiber yarn (Yarn), in which cell infiltration was revealed, was fabricated by our previously established electrospinning method.¹¹ Hyaluronate (HA) is a major component of ECM in cartilage tissue which can trigger a sophisticated signaling pathway to induce the phenotype of chondrocytes.¹² Thus, in this study, an oriented yarn mesh was established by a dynamic, liquid electrospinning method, and subsequently used as the skeleton of the freeze-dried collagen type I(Col-I)/HA chondral phase (Fig. 1). Then, using our previously fabricated, porous, beta-tricalcium phosphate (TCP) as the osseous phase, a nanofiber yarn-collagen type I/hyaluronate hybrid (Yarn-CH)/TCP biphasic scaffold was assembled by freeze drying. After combining the bone marrow mesenchymal stem cells

(BMSCs) with Yarn-CH/TCP biphasic scaffold, this tissue-engineered cartilage and the TCP complex were used to repair osteochondral defects in an animal model. Biphasic implant can allow stable fixation of the implant within the defect and repair the osteochondral defect simultaneously due to its mimetic structure. As far as we know, this is the first time for the oriented electrospun scaffold to repair *in vivo* osteochondral defect in site.

MATERIALS AND METHODS

Materials

Poly(L-lactacid)-*co*-poly(ϵ -caprolactone) P(LLA-CL) (Mw = 300 kDa; LA:CL = 75:25) was purchased from Nara Medical University, Japan. Hyaluronic acid (HA, sodium salt, Mw=0.5 MDa)

and collagen type I (Col-I) was obtained from Sigma-Aldrich Chemical Co. (St. Louis, MO) and Sichuan Ming-Rang Bio-Tech Co., China, respectively. Dulbecco's modified Eagle's medium (DMEM) and fetal bovine serum were purchased from Gibco (Grand Island, NY). All other reagents and media were of reagent grade or better and purchased from Invitrogen, unless otherwise indicated.

Fabrication of scaffolds

Fabrication of nanofiber yarn-Col-I/HA hybrid scaffold (Yarn-CH, chondral phase). The fabrication of the nanofiber yarn-collagen type I/hyaluronate hybrid scaffold (Yarn-CH), as the chondral phase, involved the combination of a dynamic, liquid electrospinning, and freeze-drying.¹³ Briefly, a water vortex was created in the basin with a hole (diameter, 8 mm) at the bottom. Then, a tank was used to deposit the drained water and then it was pumped back into the basin to maintain the water level. A solution of Col-I and P(LLA-CL) (8 wt %, Col-I:P(LLA-CL) = 10:90) in 1,1,1,3,3,3-hexafluoro-2-propanol was loaded into a syringe and fed at a feed rate of 1 mL/h with a voltage of 15 kV. A rotating mandrel (60 r/min) was used as the collector to collect the yarn by flowing along with the water through the hole. The yarn was frozen at -80°C for 6 h and then freeze-dried overnight.

For fabrication of Yarn-CH, Col-I and HA were mixed in 0.05M acetic acid to obtain the blended solution with a concentration of 1% (Col-I:HA = 1:1). Then, the yarn was immersed in the blended solution and frozen at a target temperature of -80°C for 6 h and freeze-dried overnight. Finally, the Yarn-CH was punched into dish scaffolds with a diameter of 5 mm and a height of 1 mm. As a control, the Col-I/HA solution was directly frozen at -80°C for 6 h and subsequently freeze-dried overnight to obtain a Col-I/HA sponge-like scaffold (SPONGE).

Fabrication of porous beta-TCP (osseous phase). Porous TCP cylinders (diameter 5 mm and height 5 mm) were produced by high-temperature melting method using the TCP submicron powders as in our previous study.¹⁴ Briefly, polymethylmethacrylate balls were stuck together by chemical formation as an organic skeleton in a stainless steel mold ($5 \times 5 \text{ mm}^2$ cylinder shape). Then, the skeleton was impregnated with an aqueous suspension of TCP submicron powders. After that, drying by evaporation, debinding by keeping the mold at $220\text{--}290^{\circ}\text{C}$ for about 8 h, and sintering (3 h at 1150°C) were performed to obtain the finished TCP cylinder of 5 mm diameter and 5 mm length.

Fabrication of biphasic scaffolds. For the integration of chondral phase to the osseous phase, the TCP was first pre-wetted with Col-I/HA solution (dissolved in 0.05M acetic acid; 1 wt %, Col-I:HA = 1:1) for 6 h. Thereafter, the rounded Yarn-CH was placed on the top of the porous β -TCP and frozen at -80°C for 6 h followed by overnight freeze-drying. During this process, the Col-I/HA solution was used as a cement to fix the fibrous scaffold onto the TCP. To make the chondral phase more resistant in a liquid

environment, the biphasic scaffolds were cross-linked using 1ethyl3(3dimethylaminopropyl)carbodiie hydrochloride as in our previous study.¹⁵

Characteristics of the scaffolds

Surface morphology. The surface morphology and the pore size of the chondral phase, intermediate zone, and osseous phase ($n = 5$) was determined using a Hitachi TM 1000 scanning electron microscope (SEM) at an accelerated voltage of 10 kV. All specimens were sputter coated with gold.

Mechanical testing. Stress-strain testing of the chondral phase was performed for tensile and compressive strength using a universal material tester (H5K-S, Hounsfield, UK) in the directions parallel and perpendicular to the Yarn-CH.¹⁶ Prior to the testing, all the thicknesses of the specimens were measured by a micrometer. Rectangular specimens ($30.0 \times 10.0 \text{ mm}^2$) were tested using the universal material tester with a load cell of 50N at a cross-head speed of 10 mm/min ($n = 5$).

Compressive strength was tested using a mechanical testing machine (5500R-100kN, Instron, USA) at a load cell of 1000N and a cross speed of 10 mm/min. Cylindrical specimens (5 mm in diameter and 6 mm in height, osseous phase 5 mm, and chondral phase 1 mm) were tested ($n = 5$).

Cell seeding on Yarn-CH and SPONGE

Isolation and culture of rabbit BMSCs. Animal experiments were carried out in accordance with the policies of Shanghai Jiao Tong University School of Medicine and the National Institutes of Health. Rabbit BMSCs were obtained from 16-week-old New Zealand white rabbits and further cultured as in our previous study.¹⁷ Briefly, after anesthesia by intramuscular administration of ketamine hydrochloride (60 mg/kg) and xylazine (6 mg/kg), about 5 mL of marrow was extracted from the right iliac crest by a needle, flushed with 10-mL DMEM supplemented with fetal bovine serum (10%, w/v), penicillin (100 units/mL), and streptomycin (100 mg/mL). Then, the marrow was cultured at 37°C , 5% CO_2 in a humidified incubator. The culture medium was changed after 5 days of incubation to remove the unattached cells. Third-passage cells were used for further experiment.

In vitro chondrogenesis of Yarn-CH

After sterilizing by immersion in 75% ethanol for 1.5 h and washed repeatedly with phosphate-buffered saline (PBS, pH 7.4), the scaffolds were preimmersed in culture media for 24 h to promote cell attachment. BMSCs were only seeded into chondral phase. After cell seeding with a final seeding density of 3×10^6 cells/chondral phase in each scaffold, the cell-scaffold constructs were incubated for 4 h to allow the cells to completely adhere to the scaffolds.^{17,18} Then, the constructs were incubated in the normal medium described above or a chondrogenic medium¹⁸ for 21 days. Chondrogenic medium contained 10 ng/mL TGF- β 1 (R&D), 100 nmol/L dexamethasone, 50 $\mu\text{g/mL}$ ascorbate-2-phosphate, 40 $\mu\text{g/mL}$ proline, 100 $\mu\text{g/mL}$ pyruvate (all from

Sigma), and 1:100 diluted ITS Premix (Becton Dickinson). Then, 5- μ m cross-sections from the chondral phase were obtained after fixation, dehydration, clarification, infiltration, and paraffin embedding. The sections were stained with safranin O (Sigma-Aldrich, St. Louis, MO), and images were obtained using a microscope (LEICA DM 4000 B).

***In vivo* implantation of biphasic scaffolds into osteochondral defects**

Experimental designs and surgical procedures. The *in vitro*-cultured autologous BMSCs/biphasic scaffold composites were implanted in the respective osteochondral defect of the critical-numbered rabbits as our previous method.¹⁸ The rabbits were anesthetized with both legs disinfected, as described in the previous section. A 5-cm medial parapatellar incision was made over the knee to explore the patellofemoral joint and then an osteochondral defect (diameter, 5 mm and depth, 6 mm) was created in the patellar groove of the distal femur with a hollow trephine. The implant was carefully inserted into the defect ensuring an adequate press-fit fixation until the chondral phase was flush with the articular surface. Sixty rabbits were divided into six groups according to different defect treatment: differentiated BMSCs/Yarn-CH/TCP biphasic scaffold group (group I); undifferentiated BMSCs/Yarn-CH/TCP biphasic scaffold group (group II); differentiated BMSCs/SPONGE/TCP biphasic scaffold group (group III); undifferentiated BMSCs/SPONGE/TCP biphasic scaffold group (group IV); osteochondral autograft group (group V); and untreated group (group VI). Ten joints were allocated to each group for histological analysis or mechanical evaluation, respectively. No external fixation was performed and thus the animals were allowed to move freely with total weight-loading after surgery.

Gross evaluation of regenerated tissue. Animals were euthanized by intravenous overdose of pentobarbital 12 weeks after surgery and both knees were retrieved. After opening the capsule, each joint was photographed for evaluation and then examined by the International Cartilage Repair Society (ICRS) Macroscopic Score for evaluation the degree of defect repair, integration of the border zone, and macroscopic appearance.¹⁹

Histological and immunohistochemical analyses. Ten replicate histological assessments were made for each group. After gross examination, the samples were fixed in 4% paraformaldehyde for 1 day and then decalcified in 10% EDTA for 1 month at room temperature. Samples were dehydrated through increasing concentrations of ethanol, followed by paraffin embedding. Sections were cut into 4- μ m slices and stained with Hematoxylin and eosin (H&E), toudine blue, safranin O/fast green, and Masson's trichrome. The repaired tissues were graded blindly by three observers for the overall evaluation of hyaline cartilage formation, structural characteristics, and tissue morphology in the defects, using the ICRS Visual Histological Assessment Scale.²⁰

The expression of collagen type II and I in the regenerated tissue was analyzed by immunohistological staining.

The prepared sections were dewaxed in xylene and then hydrated through graded alcohol. Endogenous peroxidase activity was blocked with 0.3% hydrogen peroxide buffered with PBS. After blocking with goat serum (Sigma) (1:100 dilution), sections were incubated with primary antibodies of collagen II (Neomarkers) and collagen I (Abcam) overnight at 4°C. After three washes in PBS, specimens were incubated with anti-mouse rabbit secondary antibodies for 1 h at 37°C. Staining was developed in 3,3'-diaminobenzidine (DAB) solution (Dako, Hamburg, Germany), with counterstaining by hematoxylin.

For detecting the TCP degradation, the samples after mechanical evaluation were embedded in polymethylmethacrylate without decalcification as in our previous method.²¹ The cross-sections were cut to about 200- μ m thickness with a Leitz Saw Microtome 1600 (Wetzlar, Germany), ground and polished to about 50 μ m thickness with an Exakt Grinder (Norderstedt, Germany). Finally, the samples were stained with Van Gieson's Picro-Fuchsin stain (V-G stain).

Mechanical evaluation. Mechanical evaluation was performed according to the instructions described previously.⁷ The compressive mechanical properties of the surface cartilage layer were tested with an Instron testing machine (model 5543; Instron) and software (Bluehill V2.0; Instron), using a 2-mm diameter cylindrical indenter fitted with a 10N maximum loading cell. The unconfined equilibrium modulus was determined by applying a step displacement (20% strain) and monitoring compressive force with time until equilibrium was reached. The thickness of the fully relaxed cartilage layer was tested to estimate strain for applied deformations. The crosshead speed used was approximately 0.06 mm/min. The ratio of equilibrium force to cross-sectional area was divided by the applied strain to calculate the equilibrium modulus (in MPa).

Statistical analysis

Descriptive statistics were used to determine group means and standard deviations for numerical data, and analysis was performed using Newman-Keuls test for multiple comparisons. Statistical significance was defined as a *p*-value <0.05.

RESULTS

Scaffold characterization

Both Yarn-CH and SPONGE were prepared in the shape of a cylinder of the same size by combining with TCP. SEM images showed obvious different microstructure in the two groups [Fig. 2(A-J)]. It was observed that in the Yarn-CH group the chondral phase had porous surface structures composed of aligned Yarn-CH and a honeycomb-like matrix. Opened and interconnected pores bound by the Yarn and matrix could be found, implying that the chondral phase had a well-designed three-dimensional structure. In the non-oriented porous group, the SPONGE only presented a randomly arranged porous structure without paralleled Yarn penetrating the matrix. Desirable bonding between the two

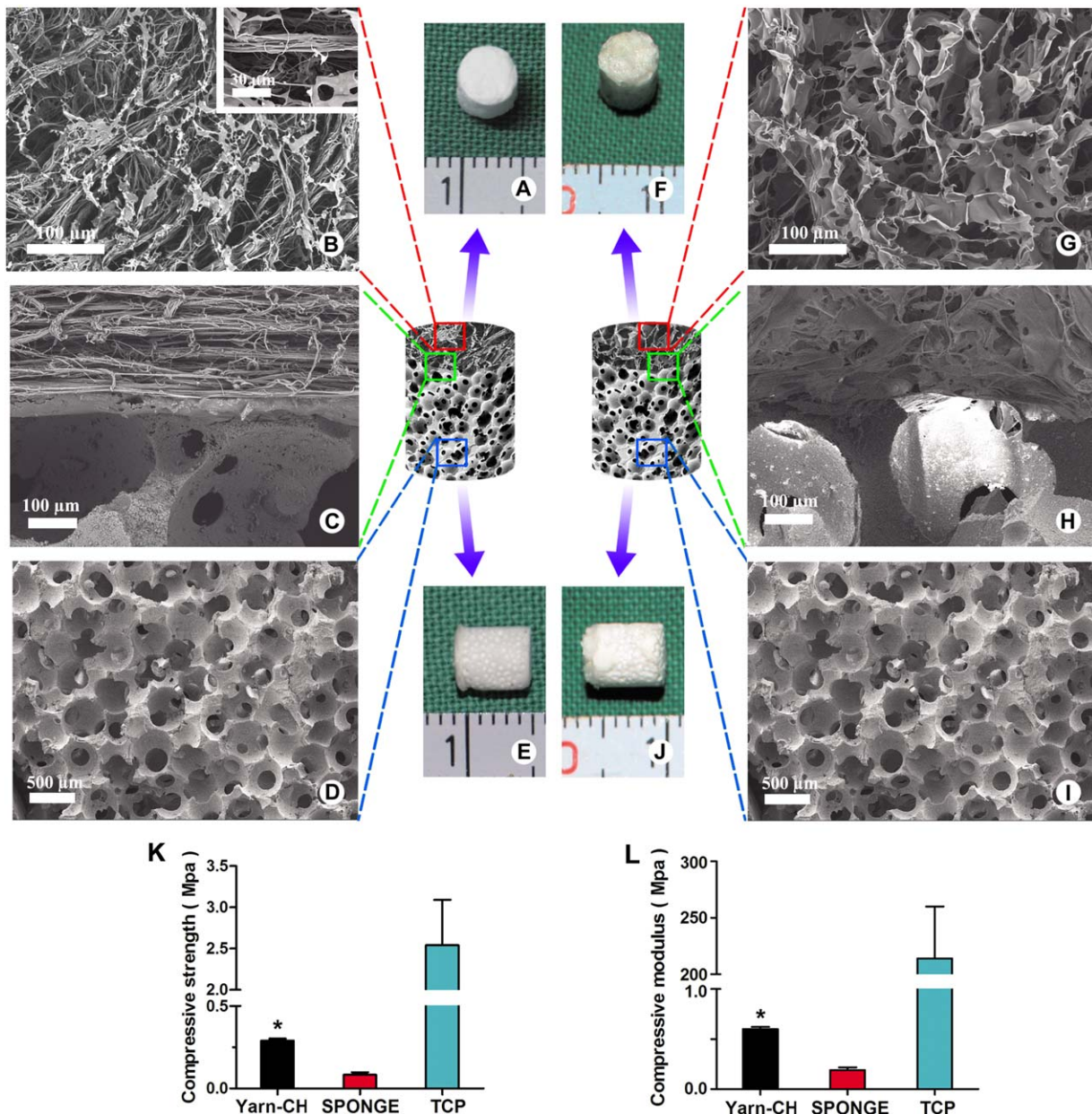


FIGURE 2. Gross observations of Yarn-CH/TCP biphasic scaffold (A, E) and SPONGE/TCP biphasic scaffold (F, J). SEM showing surface morphological features of chondral phase, intermediate zone, and osseous phase of Yarn-CH/TCP biphasic scaffold (B)–(D) and SPONGE/TCP biphasic scaffold (G)–(I), respectively. Compressive strength (K) and compressive modulus (L) of Yarn-CH, SPONGE and TCP, respectively. * $P < 0.05$ compared with SPONGE. [Color figure can be viewed in the online issue, which is available at wileyonlinelibrary.com.]

phases using collagen/hyaluronic acid as adhesive was demonstrated in Figure 2.

Mechanical loading, (one of the most important criterions to estimate scaffold function) was conducted. We considered that chondral phase would resist both compressive and tensile forces; stress-strain testing of the chondral phase on perpendicular and parallel directions was performed. Although the direction of fibers was perpendicular to the compressive forces, the compressive strength of the Yarn-CH group was threefold greater than that of the SPONGE group. The compressive strength and modulus of

Yarn-CH, SPONGE, and TCP were demonstrated in Figure 2(K,L), respectively. The Yarn-CH chondral phase had a tensile strength of 3.43 ± 0.15 MPa which was significantly higher compared to that of 1.07 ± 0.23 MPa in the SPONGE chondral phase ($p < 0.05$).

Chondrogenic differentiation

After 3 weeks of *in vitro* culture, the cells evenly distributed throughout the chondral phases in all groups. Safranin O staining was carried out to determine the production of ECM [Fig. 3(A–D)]. The constructs in the Yarn-CH group

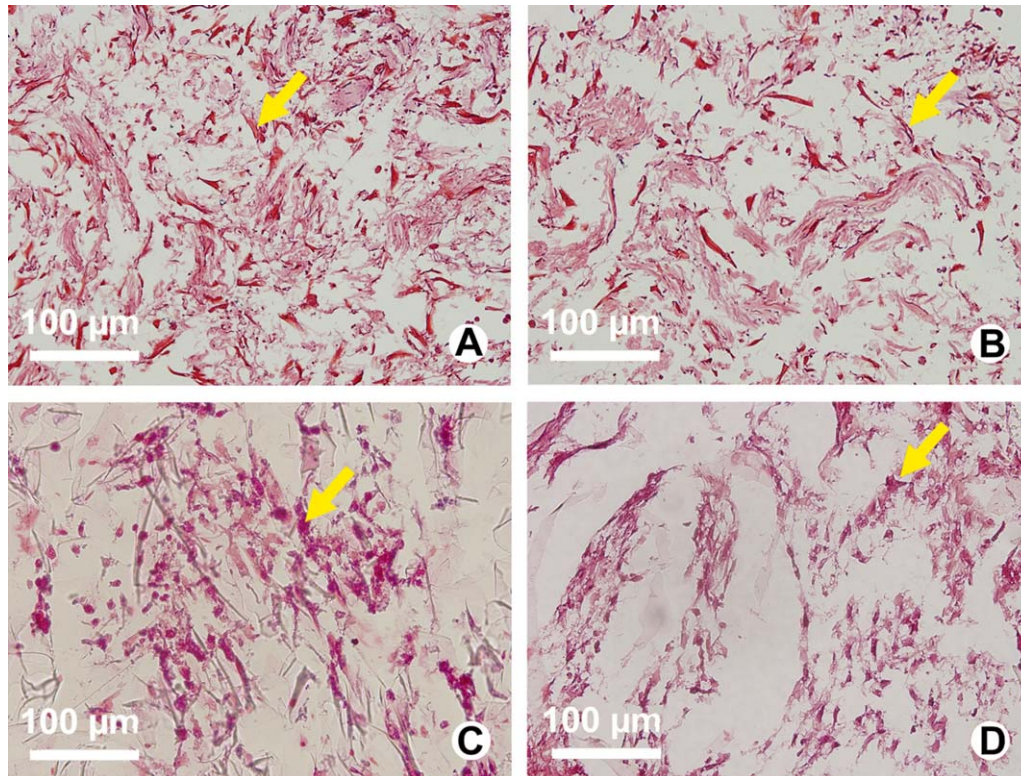


FIGURE 3. Safranin O staining from the specimens cultured for 21 days in chondrogenic differentiation medium on YARN-CH (A) and SPONGE (C) and in the normal growth medium on YARN-CH (B) and SPONGE (D). Yellow arrows indicate the cells. [Color figure can be viewed in the online issue, which is available at wileyonlinelibrary.com.]

formed a relatively homogeneous structure and ECM was observed in both outer and inner regions of the Yarn group, while ECM and relatively loose structure was discovered in the SPONGE group.

Macroscopic observations

The general health of the rabbits is good and there are no infections. The animals were totally weight-bearing, although no special protocol of the exercises was given. The free movement of the rabbits was certificated by the animal keepers. An osteochondral defect 5 mm in diameter and 6-mm deep was created. Altogether, six groups were divided for the defect repair (Fig. 4). In differentiated BMSCs/Yarn-CH/TCP biphasic scaffold group, the regenerated defects showed an almost smooth articulating surface compared with the normal cartilage in the periphery [Fig. 5(A)]. The original defect in differentiated BMSCs/SPONGE/TCP biphasic scaffold group had become full of hyaline-like repaired tissue that appeared to be integrated with the surrounding tissues [Fig. 5(C)]. In undifferentiated BMSCs/Yarn-CH/TCP biphasic scaffold [Fig. 5(B)] and undifferentiated BMSCs/SPONGE/TCP biphasic scaffold groups [Fig. 5(D)], defects were almost completely covered by rough tissue with irregular surfaces which were clearly distinguishable from the normal cartilage. In the osteochondral autograft group, the osteochondral fragments in the defect were similar to surrounding cartilage but the entire implants were slightly

depressed [Fig. 5(E)]. Macroscopic observations at 12 weeks after surgery in the untreated group revealed incomplete filling and concave defects with some regenerated tissue seen at peripheral regions [Fig. 5(F)]. The average ICRS Macroscopic Scores of each group at 12 weeks were summarized in Figure 6(A). The average scores in the differentiated or undifferentiated BMSCs/Yarn-CH/TCP biphasic group were higher than the differentiated or undifferentiated BMSCs/SPONGE/TCP biphasic groups, respectively.

Histological findings

In the differentiated BMSCs/YARN-CH/TCP biphasic scaffold group, the articular surface of the defect was repaired with cartilage-like tissue. The cell distribution and cell morphology in the regenerated cartilage were almost identical to the native host cartilage including the superficial zone [Fig. 7(A1–A4)]. Furthermore, there was good integrity of the cartilage at the host cartilage–implant interface. The subchondral space was filled with mature spongy bone, although residual materials were revealed under the subchondral tissues. Cartilage regeneration can also be detected in the undifferentiated BMSCs/YARN-CH/TCP biphasic scaffold group. However, it was lack of impregnated chondrocytes and slightly depressed with fibrous tissue in the upper part of defect, leaving an incomplete integrity of the cartilage at the host cartilage–implant interface [Fig. 7(B1–B4)]. In the differentiated BMSCs/SPONGE/TCP biphasic

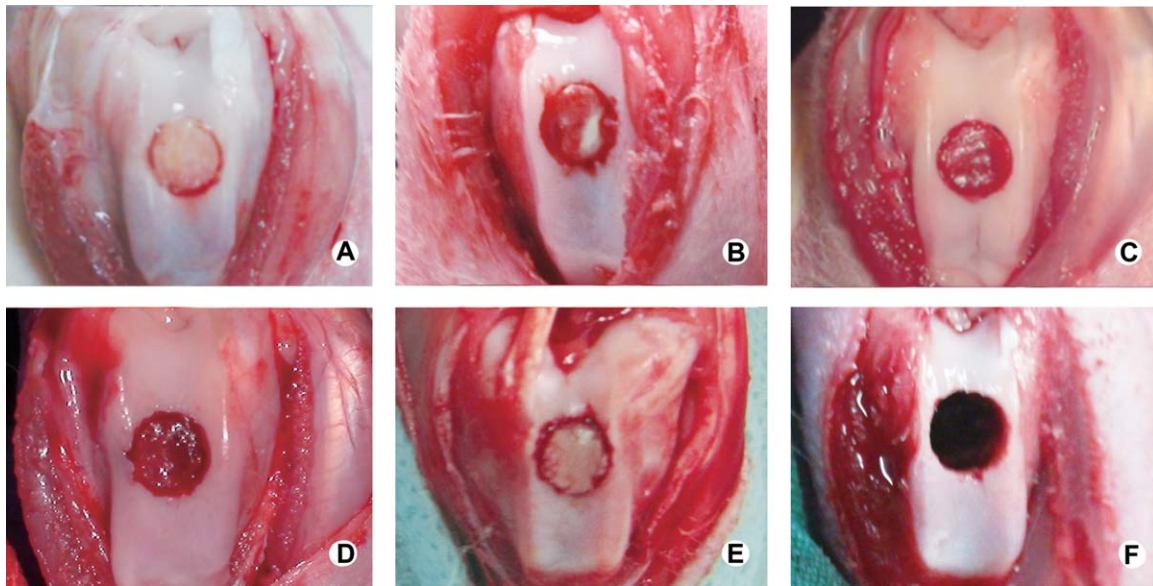


FIGURE 4. The pictures are taken at implantation and the time at implantation is defined as time 0. The defects filled with differentiated BMSCs/Yarn-CH/TCP biphasic scaffold (A); undifferentiated BMSCs/Yarn-CH/TCP biphasic scaffold (B); differentiated BMSCs/SPONGE/TCP biphasic scaffold (C); undifferentiated BMSCs/SPONGE/TCP biphasic scaffold (D); autologous osteochondral fragments (E); and the defect without treatment (F). [Color figure can be viewed in the online issue, which is available at wileyonlinelibrary.com.]

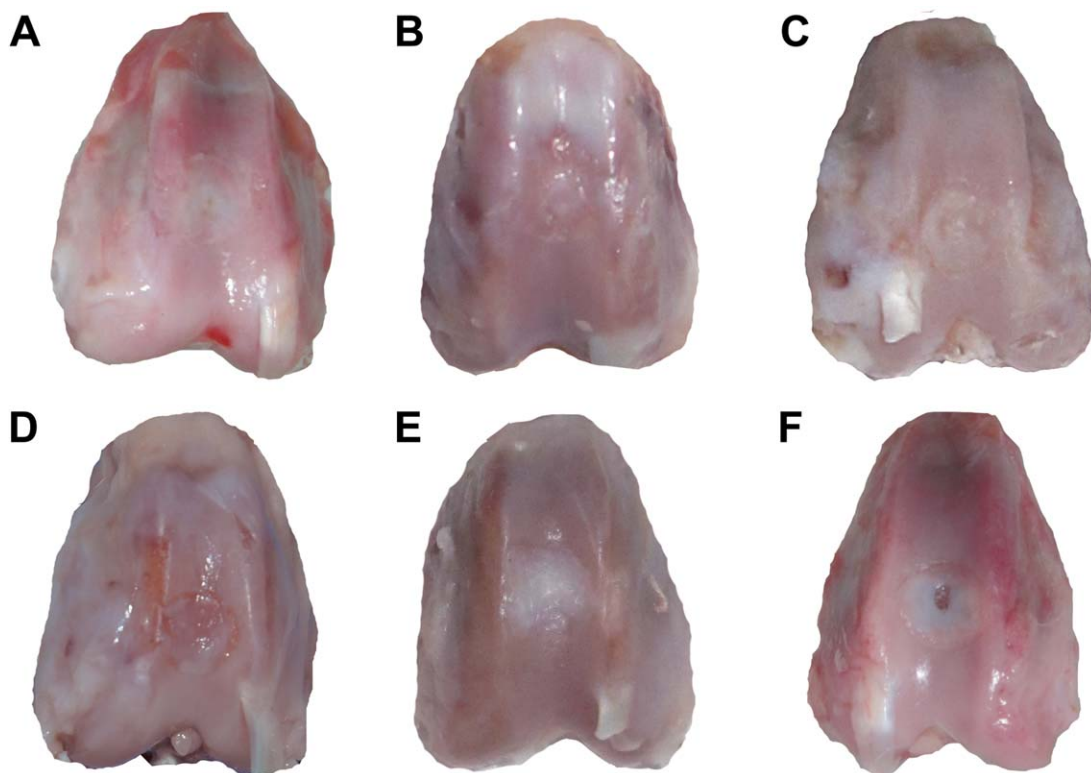


FIGURE 5. Macroscopic appearance of osteochondral defect healing in the six groups at week 12 (A–F) after surgery. Differentiated BMSCs/Yarn-CH/TCP biphasic scaffold group [(A), group I]; undifferentiated BMSCs/Yarn-CH/TCP biphasic scaffold group [(B), group II]; differentiated BMSCs/SPONGE/TCP biphasic scaffold group [(C), group III]; undifferentiated BMSCs/SPONGE/TCP biphasic scaffold group [(D), group IV]; autologous osteochondral fragments group [(E), group V] and the defect without treatment [(F), group VI]. [Color figure can be viewed in the online issue, which is available at wileyonlinelibrary.com.]

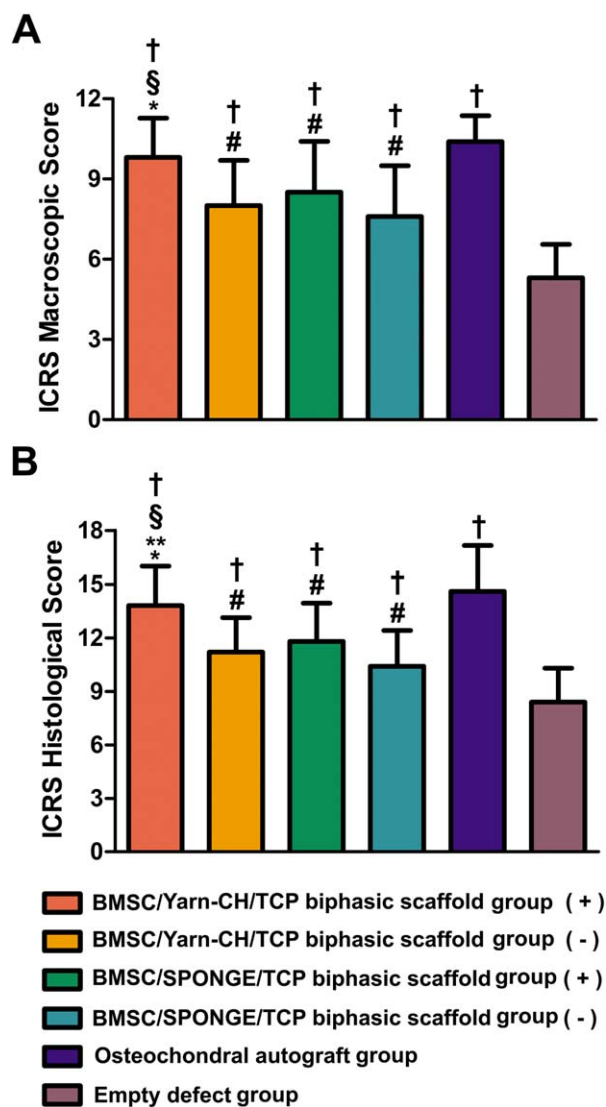


FIGURE 6. The ICRS macroscopic scores and ICRS visual histological assessment scales are shown in (A) and (B), respectively. Data are expressed as mean \pm SD (each group, $n = 10$). * $p < 0.05$ compared with undifferentiated BMSCs/Yarn-CH/TCP biphasic scaffold group; ‡ $p < 0.05$ compared with undifferentiated BMSCs/SPONGE/TCP biphasic scaffold group; ** $p < 0.05$ compared with differentiated BMSCs/SPONGE/TCP biphasic scaffold group; # $p < 0.05$ compared with osteochondral autograft group; † $p < 0.05$ compared with the defect without treatment. + and - indicate the differentiated and undifferentiated BMSCs, respectively. [Color figure can be viewed in the online issue, which is available at wileyonlinelibrary.com.]

scaffold group, the defects repaired by implants had a relatively smooth surface and were well integrated with the host cartilage; however, both safranin O and Massion's staining detected the presence of glycosaminoglycan (GAG) at low levels in the middle of the defects [Fig. 7(C1–C4)]. The defect initially filled with undifferentiated-BMSCs/SPONGE/TCP [Fig. 7(D1–D4)] biphasic scaffold was gradually replaced by a newly formed mixture of fibrous tissue and cartilage-like tissue; the integrity of the cartilage at the host cartilage–implant interface was irregular and sometimes concave areas could be observed in the center of the surfa-

ces of the defects. In the group receiving the autologous osteochondral fragments, the defects were covered by thickened cartilage and cartilaginous tissue could be detected to invaginate inside the cavities [Fig. 7(E1–E4)], which were not well-integrated with the host cartilage. The defects of the untreated group at 12 weeks were filled with fibrous tissue and remained concave, safranin O and Masson's staining was faintly observed at the center of regenerated tissues and there was no integration of the edges of the regenerated tissue with the adjacent normal cartilage or reconstitution of the subchondral bone [Fig. 7(F1–F4)]. The integrity of the cartilage at the host cartilage–implant interface was poor. In all scaffold implantation groups, subchondral bone was well-formed and bridged over the defects. TCP did not degrade completely after implantation for 12 weeks, which indicated incomplete ossification at that time. It was noted that TCP degraded equally in these groups; however, TCP could serve as a bone substitute for subchondral bone regeneration [Fig. 7(A5–F5)]. The host cartilage and the host cartilage–implant interface were shown in Figure 8(A–E) with higher magnification.

Immunohistochemical staining of sections with type II collagen antibodies showed the proteins in the regenerated tissue stained positive for type II collagen. Staining was especially smoother and more uniform in the BMSCs/Yarn-CH/TCP biphasic scaffold group than in the other groups, and the positive staining regions in each group were similar with those in safranin O staining (Fig. 9). Col-I, one osteogenic marker, was also detected; the densely stained bony areas and slightly stained cartilage regions were just opposite to collagen II staining. The ICRS Visual Histological Assessment Scale was used to evaluate the immunohistochemical staining and the average scores are shown in Figure 6(B).

Mechanical evaluation

From the indentation test, Young's modulus of repaired tissues tissue from all the groups (12 weeks) was determined and compared (Fig. 10). The compressive modulus of the repaired tissue in the differentiated-BMSCs/YARN-CH/TCP biphasic scaffold group (0.27 ± 0.09 MPa) showed greater improvement than specimens from the other matrix implanting groups, except in the osteochondral autograft group (0.38 ± 0.21 MPa). The repaired tissue in the undifferentiated-BMSCs/YARN-CH/TCP biphasic scaffold group (0.20 ± 0.077 MPa), the undifferentiated-BMSCs/SPONGE/TCP biphasic scaffold group (0.19 ± 0.1 MPa), and the differentiated-BMSCs/SPONGE/TCP biphasic scaffold group (0.23 ± 0.13 MPa) showed similar mechanical data without significant differences, and the modulus of repaired tissue in the untreated group (0.096 ± 0.078 MPa) was inferior to all the other groups.

DISCUSSION

The techniques of dynamic liquid electrospinning and freeze-drying utilized in this study offer a new approach to the fabrication of chondral scaffolds with enhanced

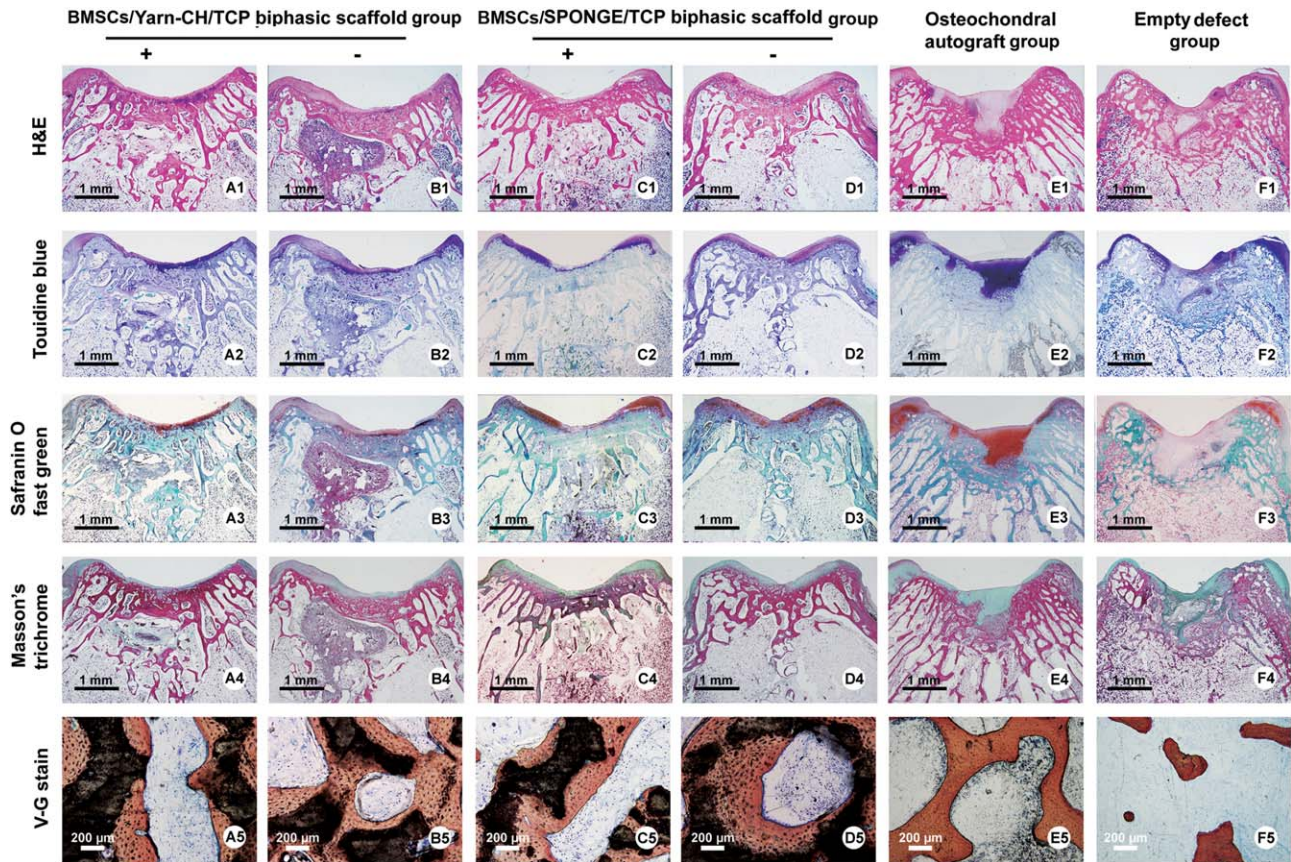


FIGURE 7. H&E(A1-F1), toudine blue(A2-F2), safranin O/fast green(A3-F3), Masson's trichrome(A4-F4), and V-G stain(A5-F5) of sections from six groups at 12 weeks after surgery. + and – indicate the differentiation and undifferentiation of BMSCs, respectively. [Color figure can be viewed in the online issue, which is available at wileyonlinelibrary.com.]

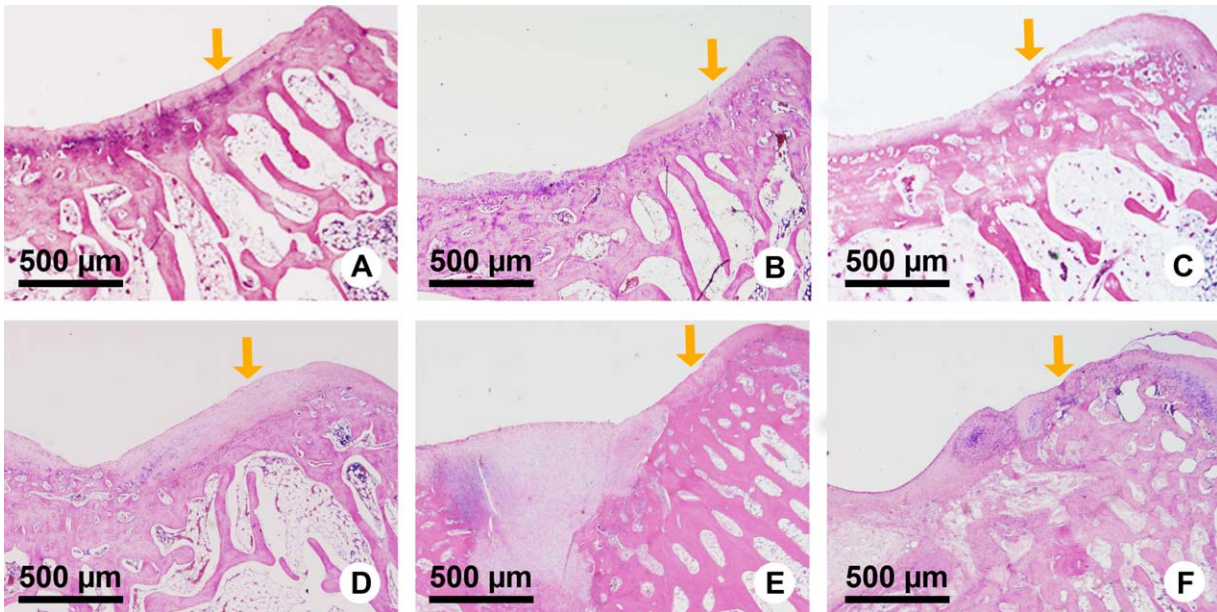


FIGURE 8. Histological examination of the cartilage repaired by differentiated BMSCs/Yarn-CH/TCP biphasic scaffold group (A), undifferentiated BMSCs/Yarn-CH/TCP biphasic scaffold group (B), differentiated BMSCs/SPONGE/TCP biphasic scaffold group (C), undifferentiated BMSCs/SPONGE/TCP biphasic scaffold group (D), autologous osteochondral fragments group (E), and the defect without treatment group (F) is shown with higher magnification. The host cartilage–implant interface is indicated with yellow arrows in each image. [Color figure can be viewed in the online issue, which is available at wileyonlinelibrary.com.]

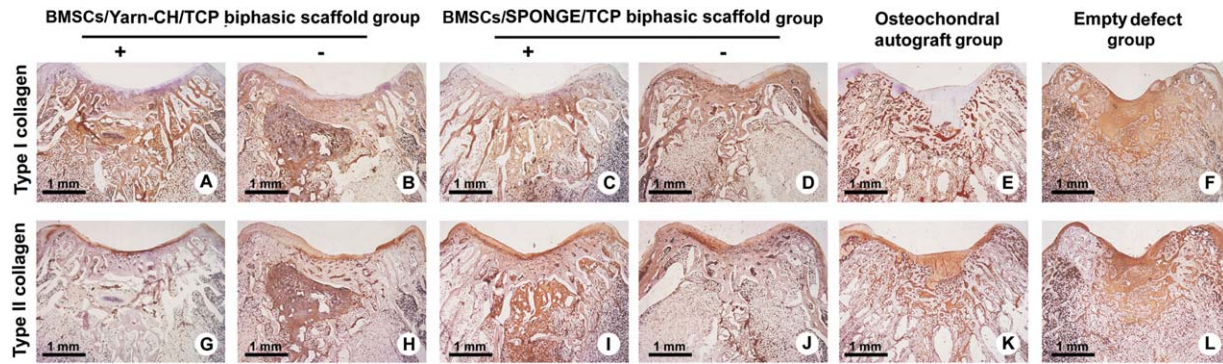


FIGURE 9. Type II collagen (A)–(F) and type I collagen (G)–(L) immunohistological staining of sections from the six groups at 12 weeks after surgery. + and – indicate the differentiation and undifferentiation of BMSCs, respectively. [Color figure can be viewed in the online issue, which is available at wileyonlinelibrary.com.]

mechanical properties and subsequently to dealing with osteochondral defects. Nanofiber yarn-collagen type I/hyaluronate hybrid scaffold (Yarn-CH) can serve as chondral phases to allow the infiltration of MSCs. The combination of BMSCs, tissue-engineered Yarn-CH, and TCP complex was successfully used to repair the osteochondral defects in the rabbit model with an improved compressive modulus.

In this study, the Yarn-CH as the chondral phase of biphasic scaffold had a distinctly stratified structure with enhanced compressive strength due to the addition of Yarn as skeleton in SPONGE. Previously, the sponge scaffolds with components of atelocollagen and hyaluronate were used to facilitate the attachment and growth of chondrocytes.¹⁷ However, such scaffolds were fabricated by freeze-drying and chemical cross-linking of collagen-based materials and thus the compressive strength was only 0.075 MPa.^{22,23} In this study, the Yarn was placed within the Col I/HA matrix for fiber reinforcement. As a result, the compressive strength of the Yarn-CH group was threefold greater than that of the SPONGE group. Furthermore, the tensile strength in the Yarn-CH was threefold greater than in the SPONGE ($P < 0.05$). This is similar to the principle of reinforced concrete, in which steel bars within the structure improve the tensile strength of the concrete.

The *in vivo* fate is the most important criterion for evaluating the final cartilage formation. The current results demonstrated that oriented Yarn-CH promoted better *in vivo* cartilage formation than did the SPONGE. The implantation of Yarn-CH with differentiated-BMSCs showed superior cartilage formation with predominant GAG deposition and bridged the patellar groove defect by repairing the cartilage. The cartilage healing also means better functional restoration of mechanical loading. The healing effect in the differentiated-BMSCs/SPONGE/TCP biphasic scaffold group was inferior given the prevalence of fibrocartilage and lower GAG distribution within and beyond the defect. Interestingly, the morphological observations at the patellar groove were similar for the BMSCs/SPONGE/TCP biphasic scaffold groups, when the BMSCs were undifferentiated, a high incidence of fibrocartilage was found with less positive staining of collagen II and it was accompanied by GAG depletion at

the repair sites of both groups. Although natural grafting is a source of cartilage and bone, donor-site morbidity and age-dependent quality have been of concern. Graft harvesting entails extra damage, which is painful and inflicts scarring. In addition, the placing back cartilage was excessively thick although remained a high GAG deposition. To some extent, high GAG deposition can explain the advanced functional restoration of mechanical loading. TCP is a biomaterial similar to bone mineral constitution with good biocompatibility and osteoconductivity.²⁴ After the work done in this study, it was presumed that the BMSCs can be recruited from the bone marrow and surrounding areas into the TCP because the BMSC's impact on bone regeneration seems to be negligible according to our findings. All the

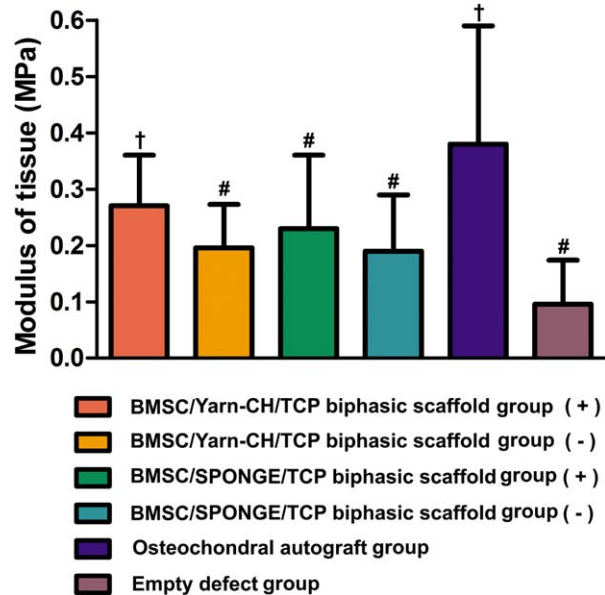


FIGURE 10. The relative Young's modulus of repaired tissues from all the groups after 12 weeks. # $p < 0.05$ compared with osteochondral autograft group; † $p < 0.05$ compared with the defect without treatment. + and – indicate the differentiation and undifferentiation of BMSCs, respectively. [Color figure can be viewed in the online issue, which is available at wileyonlinelibrary.com.]

scaffold implanting groups showed similar subchondral bone union and TCP degrading process in the osseous phase, which occurred in the same way as in the previous study.²⁵

The cartilage was regenerated in the new areas with enhanced compressive strength. Despite of the enhanced mechanical properties of Yarn-CH, the structural bionic may be another reason. It is known that normal articular cartilage consists of four different zones. The superficial zone of naturally functioning articular cartilage, a very polarized, dense organization of fibrils are oriented parallelly to the plane of the articular surface.^{26,27} Thus, the Yarn-CH may reproduce certain cartilaginous structure cues, especially within the superficial zone. However, the deep zone with a longitudinally oriented structure takes the most important responsibility in distributing loads and resisting compression. So, the scaffold design of longitudinally oriented structure mimicking the deep zone of the articular cartilage should be performed. Nevertheless, this study did investigate the fate of *in vitro* engineered cartilage based on oriented scaffolds in an animal model, especially the *in vivo* results of the engineered superficial zone of the articular cartilage, which may give supportive data for further design and study. The respect effect of compressive strength and structural bionic should be investigated in further study. In addition, no measure of pore size and porosity was made, which is definitely a limitation of this study, and the measure should be detected in further study.

CONCLUSIONS

Electrospun P(LLA-CL) nanofiber yarn (Yarn) can be fabricated by a dynamic liquid supporting system for subsequent application into a freeze-dried collagen type I/hyaluronate sponge scaffold to form the chondral phase of the biphasic scaffold for osteochondral defect. Using Yarn as skeleton, a more ideal mechanical strength of the freeze-dried collagen type I(Col-I/hyaluronate (HA) sponge scaffold (SPONGE) can be maintained than with only the SPONGE itself. Our *in vitro* results show that such Yarn Col-I/HA hybrid scaffold can accommodate the cells like SPONGE. After combination of BMSCs, tissue engineered Yarn-CH and TCP biphasic complex was successfully used to regenerate the osteochondral defects in the rabbit model with greatly improved compressive modulus.

ACKNOWLEDGMENT

The authors would like to thank Dr. KR Dai, Dr. GW Liu, Dr. WG Cui, and Dr. TT Tang for their excellent technical assistance.

REFERENCES

- Smyth NA, Haleem AM, Murawski CD, Do HT, Deland JT, Kennedy JG. The effect of platelet-rich plasma on autologous osteochondral transplantation in an *in vivo* rabbit model. *J Bone Joint Surg Am* 2013;95A:2185–2193.
- Case ND, Duty AO, Ratcliffe A, Muller R, Guldberg RE. Bone formation on tissue-engineered cartilage constructs in vivo: Effects of chondrocyte viability and mechanical loading. *Tissue Eng* 2003; 9:587–596.
- Li X, Su G, Wang J, Zhou Z, Li L, Liu L, Guan M, Zhang Q, Wang H. Exogenous bFGF promotes articular cartilage repair via up-regulation of multiple growth factors. *Osteoarthritis Cartilage* 2013;21:1567–1575.
- Chotel F, Knorr G, Simian E, Dubrana F, Versier G, French Arthroscopy S. Knee osteochondral fractures in skeletally immature patients: French multicenter study. *Orthop Traumatol Surg Res* 2011;97:S154–S159.
- Versier G, Dubrana F, French Arthroscopy S. Treatment of knee cartilage defect in 2010. *Orthop Traumatol Surg Res* 2011;97: S140–S153.
- Tibesku CO, Szuwart T, Kleffner TO, Schlegel PM, Jahn UR, Van Aken H, Fuchs S. Hyaline cartilage degenerates after autologous osteochondral transplantation. *J Orthop Res* 2004; 22:1210–1214.
- Zhou GD, Liu W, Cui L, Wang XY, Liu TY, Cao YL. Repair of porcine articular osteochondral defects in non-weightbearing areas with autologous bone marrow stromal cells. *Tissue Eng* 2006;12: 3209–3221.
- Duan X, Zhu XD, Dong XX, Yang J, Huang FG, Cen SQ, Leung F, Fan HS, Xiang Z. Repair of large osteochondral defects in a beagle model with a novel type I collagen/glycosaminoglycan-porous titanium biphasic scaffold. *Mater Sci Eng C Mater Biol Appl* 2013; 33: 3951–3957.
- Jiang CC, Chiang H, Liao CJ, Lin YJ, Kuo TF, Shieh CS, Huang YY, Tuan RS. Repair of porcine articular cartilage defect with a biphasic osteochondral composite. *J Orthop Res* 2007;25:1277–1290.
- Ho STB, Huttmacher DW, Ekaputra AK, Hitendra D, Hui JH. The evaluation of a biphasic osteochondral implant coupled with an electrospun membrane in a large animal model. *Tissue Eng Part A* 2010;16:1123–1141.
- Wu J, Liu S, He L, Wang H, He C, Fan C, Mo X. Electrospun nanoYarn-CH scaffold and its application in tissue engineering. *Mater Lett* 2012;89:146–149.
- Chow G, Knudson CB, Homandberg G, Knudson W. Increased expression of CD44 in bovine articular chondrocytes by catabolic cellular mediators. *J Biol Chem* 1995;270:27734–27741.
- Mandal BB, Kundu SC. Cell proliferation and migration in silk fibroin 3D scaffolds. *Biomaterials* 2009;30:2956–2965.
- Zhang F, Lin K, Chang J, Lu J, Ning C. Spark plasma sintering of macroporous calcium phosphate scaffolds from nanocrystalline powders. *J Eur Ceram Soc* 2008;3:539–545.
- Park S-N, Lee HJ, Lee KH, Suh H. Biological characterization of EDC-crosslinked collagen-hyaluronic acid matrix in dermal tissue restoration. *Biomaterials* 2003;24:1631–1641.
- Zhang KH, Wang HS, Huang C, Su Y, Mo XM, Ikada Y. Fabrication of silk fibroin blended P(LLA-CL) nanofibrous scaffolds for tissue engineering. *J Biomed Mater Res Part A* 2010;93A:984–993.
- Im GI, Ahn JH, Kim SY, Choi BS, Lee SW. A Hyaluronate-atelocollagen/beta-tricalcium phosphate-hydroxyapatite biphasic scaffold for the repair of osteochondral defects: A porcine study. *Tissue Eng Part A* 2010;16:1189–1200.
- Cao L, Yang F, Liu GW, Yu DG, Li HW, Fan QM, Gan Y, Tang T, Dai K. The promotion of cartilage defect repair using adenovirus mediated Sox9 gene transfer of rabbit bone marrow mesenchymal stem cells. *Biomaterials* 2011;32:3910–3920.
- Jiang YZ, Chen LK, Zhu DC, Zhang GR, Guo C, Qi YY, Ouyang HW. The inductive effect of bone morphogenetic protein-4 on chondral-lineage differentiation and *in situ* cartilage repair. *Tissue Eng Part A* 2010;16:1621–1632.
- Mainil-Varlet P, Aigner T, Brittberg M, Bullough P, Hollander A, Hunziker E, Kandel R, Nehrer S, Pritzker K, Roberts S, Stauffer E; International Cartilage Repair Society. Histological assessment of cartilage repair: A report by the Histology Endpoint Committee of the International Cartilage Repair Society (ICRS). *J Bone Joint Surg Am* 2003;85A:45–57.
- Xie YZ, Chopin D, Morin C, Hardouin P, Zhu ZN, Tang JA, Lu J. Evaluation of the osteogenesis and biodegradation of porous biphasic ceramic in the human spine. *Biomaterials* 2006;27:2761–2767.
- Gotterbarm T, Richter W, Jung M, Vilei SB, Mainil-Varlet P, Yamashita T, Breusch SJ. An *in vivo* study of a growth-factor enhanced, cell free, two-layered collagen-tricalcium phosphate in deep osteochondral defects. *Biomaterials* 2006;27:3387–3395.

23. Ahn JH, Lee TH, Oh JS, Kim SY, Kim HJ, Park IK, Choi BS, Im GI. A novel hyaluronate-atelocollagen/beta-TCP-hydroxyapatite biphasic scaffold for the repair of osteochondral defects in rabbits. *Tissue Eng Part A* 2009;15:2595–2604.
24. Gan YK, Dai KR, Zhang P, Tang TT, Zhu ZN, Lu JX. The clinical use of enriched bone marrow stem cells combined with porous beta-tricalcium phosphate in posterior spinal fusion. *Biomaterials* 2008;29:3973–3982.
25. Schaefer D, Martin I, Jundt G, Seidel J, Heberer M, Grodzinsky A, Bergin I, Vunjak-Novakovic G, Freed LE. Tissue-engineered composites for the repair of large osteochondral defects. *Arthritis Rheum* 2002; 46:2524–2534.
26. Wise JK, Yarin AL, Megaridis CM, Cho M. Chondrogenic differentiation of human mesenchymal stem cells on oriented nanofibrous scaffolds: Engineering the superficial zone of articular cartilage. *Tissue Eng Part A* 2009;15:913–921.
27. Zhang Y, Yang F, Liu K, Shen H, Zhu Y, Zhang W, Liu W, Wang S, Cao Y, Zhou G. The impact of PLGA scaffold orientation on in vitro cartilage regeneration. *Biomaterials* 2012;33:2926–2935.